Emission-angle-dependent post-collision interaction

P. W. Arcuni*
Physics Division, Argonne National Laboratory, Argonne, Illinois 60439
and Physics Department, University of Chicago, Chicago, Illinois 60637
(Received 24 June 1985)

We studied the autoionization electrons of two doubly excited states of helium—$(2s\,2p)^1P$ and $(2p^2)^1D$—that were collisionally excited by multiply charged and relatively fast ions. The ion velocities (2—4.5 a.u.) were faster than the velocities of the emitted electrons (~ 1.6 a.u.). The wings of the measured autoionization profiles were significantly different from standard Beutler-Fano profiles. These differences are largest at forward angles, smaller ion velocities, and larger ion charges. The distortion is explained with use of a classical kinematic model. After emission, the autoionization electron is accelerated if emitted in a forward direction (toward the projectile) or slowed down if emitted in a backward direction (away from the projectile). A modification of a post-collision interaction theory accounts for the interference between the bound-state electrons and the continuum electrons. Fits of the measured electron-energy spectra with use of this model show very good agreement.

I. INTRODUCTION

The spectral line shape of electrons emitted from autoionizing states of neutral atoms, after excitation by multiply charged ions, has received much attention over the past 20 years. Barker and Berry[1] were the first to comment on broadening and energy shifts of such profiles due to slowly moving charged particles. This effect is now called "post-collision interaction," or PCI.[2–7] Various other related effects, such as line broadening due to the recoil of the emitting atom, have also been discussed.[8–11] There have also been experimental studies at high projectile velocities[12–17] and some theoretical analyses.[18,19] Interference between the discrete states and the continuum, and between the discrete states themselves, is important in both kinematic regimes. This has been discussed by Fano,[20] who applied it to inelastic electron scattering, and was later applied to electron emission by Balashov and his group.[21,22]

At higher projectile velocities (greater than 1.0 a.u.) the influence of the ionic projectile on the continuum states (as represented by "charge exchange to the continuum"[23,24]) and the resulting effect on the interference behavior has been discussed.[19] Some writers have commented on the possible importance of the excitation process itself on the line profiles.[18,19] It has always been assumed, however, that an electron emitted in the decay process and which is moving more slowly than the charged projectile will be negligibly affected by the field of that projectile. Such an assumption does not consider the long-range nature of the Coulomb force and the strong effect that it would have on a free electron. This paper presents both the experimental observation and theoretical analysis of such an effect on the decays of the $(2p^2)^1D$ and $(2s2p)^1P$ autoionizing states of neutral helium.

II. EXPERIMENT

High-energy He^{n+} $(n=1,2)$ and Li^{n+} $(n=1,2,3)$ ions were produced by using foil and gas strippers after they were accelerated by the Argonne National Laboratory 4.5-MV Dynamitron Accelerator. The ion beam was collimated to a diameter of 2 mm. The target was a helium gas jet. When the target gas flow was off, the residual pressure was about 4×10^{-7} Torr; when it was on, the background pressure was 2×10^{-4} Torr. The pressure at the target was determined to be about 4 times the background pressure. Several tests demonstrated that few charge-changing collisions of the ion beam occurred.

Two 45°, parallel-plate electrostatic spectrometers were used to energy-analyze the electrons emitted from the target. The characteristics of this spectrometer design are fully discussed in other publications.[25,26] We obtained a resolution of 0.1 eV full width at half maximum (FWHM) by using deceleration grids located at the entrance of each spectrometer. The resolution was confirmed through the measurement of autoionization lines of known widths.

The electrons were detected by electron multipliers directly attached to the spectrometers. The signal intensity was linearly proportional to the measured background pressure. This would indicate that during the ~ 15-cm total path length the electrons experienced few inelastic or large-angle elastic collisions with the background helium gas. There were no dark counts. It is possible for electrons to enter the spectrometers and multipliers through many unexpected routes. Such stray electrons—that do not come directly from the target—could be measured and accounted for.

A deep Faraday cup collected the ion beam and the total charge was integrated to normalize the beam exposure of each data point. The signals were amplified and digitally counted. Nearly all of the experimental parameters

could be controlled through an on-line PDP-11/45 computer, where the data were recorded into a multichannel scaling mode. Metal surfaces inside the chamber were coated by conductive graphite and the entire chamber was surrounded by μ metal.

Representative partial spectra are shown in Figs. 1–3. Each spectrum at a particular angle and ion energy took from 0.5 to 8 h. The effective spectrometer constant—the number needed to multiply the voltage difference between the two plates in order to obtain the true electron energy—was not constant over a period of several hours. This was probably due to the slow accumulation of charge on various surfaces inside the spectrometer. The measured electron energy could shift by as much as several tenths of an eV. It was therefore necessary to add several short runs together after making appropriate shifts in the energy scale. Absolute values for the locations of the peaks cannot be reported since no absolute determination of the energy scale was made.

The energy step size depended on the spectral features being measured. For background measurements far from the peaks the spectrometers were stepped every 0.1 eV. Near the peaks they were stepped every 0.05 eV. The smaller step size allowed for better visual determination of peak location, making the addition of various runs easier. The electron spectra between 37 and 41 eV were not measured in order to avoid the large number of autoionizing states that occur in that energy range.

III. MODEL AND ANALYSIS

The standard parametrization of autoionization profiles is some variant of either the Shore parameters[21,27,28] or

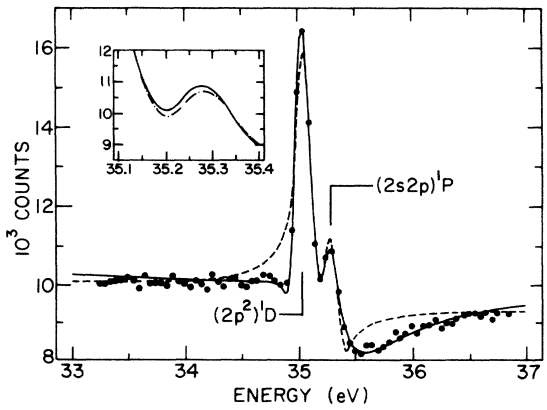

FIG. 1. Electron-energy spectrum detected at 20° from the beam direction, after 1500-keV $^7Li^{3+}$-ion collisions with neutral He. Only two autoionizing lines of He in this energy range have significant cross sections, and they are labeled. The dots are the individual data points. The dashed line is the plotted result of a least-squares fit using the Shore formula [Eq. (1) in the text]. The solid line is the plotted result of a least-squares fit using Eq. (7) in the text. This latter formula includes the Coulomb interaction between the autoionized electron and the fast lithium ion. The inset shows the possible effect of interference between the two peaks, as discussed in the text, on a very expanded scale. The solid line is the fit with no interference, and the dashed-dotted line includes a possible interference effect.

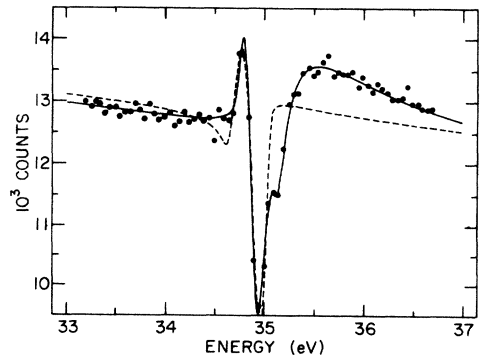

FIG. 2. Energy spectrum of electrons emitted after 1500-keV $^7Li^{3+}$ ions collided with neutral He, detected at 40° with respect to the beam direction. The significance of the points and the lines are the same as in Fig. 1.

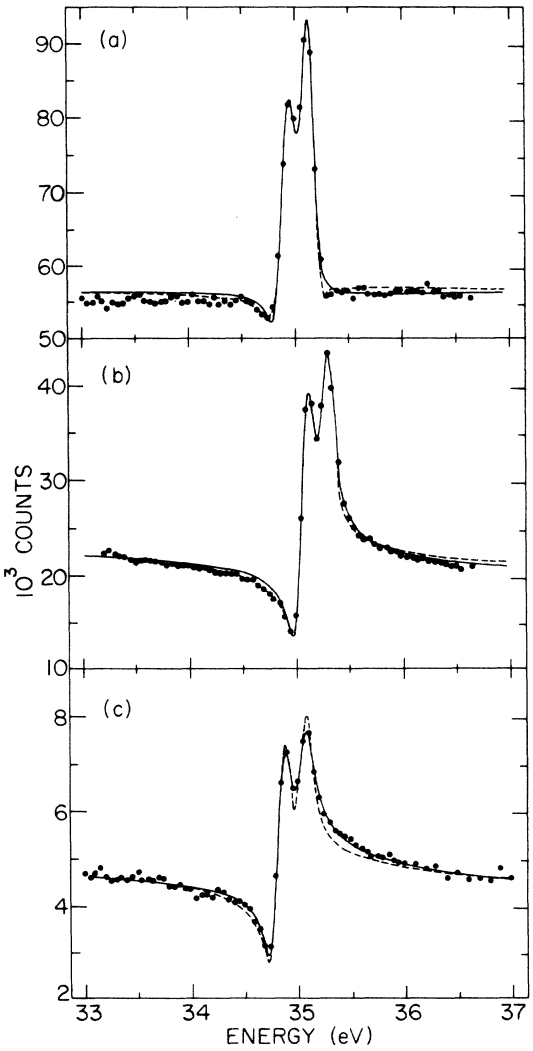

FIG. 3. (a) Electrons emitted at 30°, after 2000-keV $^4He^+$ ions collided with neutral He. (b) Electrons emitted at 30°, after 2000-keV $^4He^{2+}$ ions collided with neutral He. (c) Electrons emitted at 30° after 3500-keV $^7Li^{3+}$ ions collided with neutral He. The significance of the points and lines are the same as in Fig. 1.

the equivalent Fano formula.[20,28] Both parametrizations are identical and general—they accurately describe the interference between an isolated resonance and the continuum in which it is embedded—and can be applied to photoabsorption spectra, electron-loss measurements, and electron-emission measurements. This parametrization does not make any assumptions as to the mechanism of excitation—it does not, for instance, require the first Born approximation.[28] However, any effects due to external influences, as happens in a post-collision interaction such as the one described in this paper, are not included.

The dashed lines in Figs. 1–3 are preliminary least-squares fits of the data using the Shore parametrization,[28] in which the spectral intensity is written

$$F(\omega,\theta,E_p)=A(\omega,\theta,E_p)+\sum_r (2S_r+1) \times \frac{A_r(E_p,\theta)\varepsilon_r+B_r(E_p,\theta)}{1+\varepsilon_r^2}, \tag{1}$$

where $A(\omega,\theta,E_p)$ is the continuous background intensity, S_r is the spin quantum number of the resonance, A_r and B_r are the asymmetric and symmetric Shore parameters, both functions of the projectile energy per amu, E_p, and the observation angle θ. ε_r is the reduced energy, $\varepsilon_r=2(\omega-E_r)/\Gamma_r$, where Γ_r is the natural width of the resonance at energy E_r, and ω is the continuous energy variable. The sum is over the different resonances included in the fit. The fitting parameters in the dashed-line fit were, for both the ^1D and the ^1P peaks, the symmetric and asymmetric Shore parameters, the peak energies, and a linear background. Equation (1) was analytically folded with a triangular spectrometer acceptance function that had a FWHM of 0.1 eV. The natural linewidths for the ^1D and ^1P peaks were fixed at 0.073 and 0.039 eV, respectively.[29] It was difficult, however, to fit most of the spectra using this formula, particularly at small observation angles, small projectile velocities, and high projectile charge states. The difficulty could not be attributed to interference between the two states, which, though not included in Eq. (1), can be calculated as small for these two, presumably unperturbed, states (this will be discussed in more detail later). Indeed, some of the peak profiles are impossible to explain even qualitatively when using Eq. (1). Thus, in Fig. 1, the low-energy wing is peculiarly sharp and the high-energy wing is quite broad. The spectrum in Fig. 2 shows at least two separate oscillations through the background level, while Eq. (1) allows for only one. In Fig. 3 the spectrum produced by a He^+ beam is convincingly fitted by the Shore formula, but the spectrum produced by an equal-velocity Li^{3+} beam is not fitted as well. Kinematic broadening due to movement of the excited atom after the collision[8–10] is small at this projectile velocity[30] and displays the wrong systematics; kinematic broadening is a maximum at 90° and is a minimum at more forward and backward angles—not the effect observed. We propose instead that a form of post-collision interaction, as outlined below, explains the discrepancy between the observed line profiles and the standard Shore parametrization.

The autoionizing state decays by emitting an electron at some time, t', and at some angle, θ, relative to the beam direction. The ion that excites this state moves far before the state decays—in one lifetime of the ^1D state (about 9×10^{-6} ns) a 1500-keV ^7Li ion moves about 500 Å. Phenomena that require a small distance between the ion and the atom, such as the formation of molecular states,[31] and Stark mixing of the excited atomic states, may therefore be neglected at the time of decay. The impact parameter for excitation of an autoionizing state is small (about 4 a.u.). The distance from the ion to the autoionizing atom at time t is then approximated as $v(t-t_0)$, where v is the velocity of the ion and t_0 is the time of formation of the excited state. At the time of emission, t', the electron will experience a potential due to the moving ion of $Q[v(t'-t_0)]^{-1}$, where Q is the charge of the ion.

The classical description of an electron in the presence of two moving charges is a three-body problem, but some simplifying assumptions can be made. First, we assume that the electron is emitted at the velocity v_0, given by the undisturbed energy difference between the initial and final states. The residual helium ion is assumed to have no other influence on the kinematic situation. After conversion to the projectile frame of reference, both the kinetic and potential energies of the electron can be easily calculated, yielding a total energy

$$E_{\text{total}}=\frac{(v_0\cos\theta-v)^2+v_0^2\sin^2\theta}{2}-\frac{Q}{v(t'-t_0)}. \tag{2}$$

This total energy becomes the total kinetic energy as the ion-electron distance approaches infinity. If we assume that the electron velocity in the direction perpendicular to the ion velocity remains unchanged—this limits any partial orbiting about the ion—we can calculate the final velocity in both the ionic and laboratory reference frames. Thus the energy change of an electron emitted at a time t' and at an energy E_i becomes, in the laboratory reference frame,

$$\Delta E=\omega-E_i=v^2\left[1-R\cos\theta-\frac{Q}{v^3(t'-t_0)} - \left[(1-R\cos\theta)^2-\frac{2Q}{v^3(t'-t_0)}\right]^{1/2}\right], \tag{3}$$

where R is the ratio of the initial electronic velocity to the ionic velocity, $R=v_0/v$. Since $2Q[v^3(t'-t_0)]^{-1}$ is small, by expanding the radical one can get, to a good approximation,

$$\Delta E=\frac{Q}{v(t'-t_0)}\frac{R\cos\theta}{1-R\cos\theta}. \tag{4}$$

A plot of ΔE versus time and angle is shown in Fig. 4.

When the projectile is slow relative to the emitted electron ($v_0\gg v$), then the change in energy of the emitted electron is $\Delta E=-Q/[v(t'-t_0)]$. This is the better known model of Barker and Berry.[1] It should be noted that one does not obtain the Barker-Berry model from Eq. (4) when v gets very small. Equation (4) is not a generali-

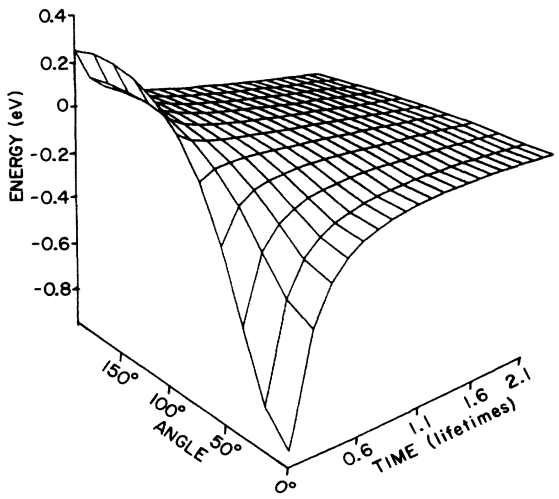

FIG. 4. Plot of the negative of the change in energy of an electron emitted from the $(2p^2)^1D$ state of He after excitation by a 1500-keV $^7Li^{3+}$ ion. This is Eq. (4) in the text plotted as a function of both emission angle and time after the formation of the state. The time is in units of the natural lifetime of the $(2p^2)^1D$ state.

zation of the Barker-Berry model, but describes a totally different kinematic regime. In the slow-projectile case the projectile is considered stationary, while the fast emitted electron is subject to its field. This assumption is the origin of the angle independence of the Barker-Berry model. In the derivation of Eq. (4), the emitted electron is instead considered stationary while it is subject to the field of the fast projectile. This is a consequence of the assumption mentioned above, that $v_0\sin\theta$ remain constant. Another way to consider this is to say that the direction vector between the electron and the projectile is always in the x direction whenever the projectile's field is significant. With the quadratic dependence of energy on velocity, ΔE is thus very small when the emitted electrons are observed at 90°.

When both the electron and the projectile move at comparable velocities, serious kinematic complications ensue. In the classical model considered here, the electron can follow Coulomb trajectories, around and by the projectile, that depend on the time and angle of emission, and models such as the one leading to Eq. (4) or the Barker-Berry model are clearly not adequate. Dahl *et al.*[9] have considered the deflection of a fast electron which is emitted toward a slowly moving ion, but their approach has only limited applicability. Numerical solutions are possible, but we suspect that a quantum-mechanical approach to the electron's motion will be more successful. In this difficult regime, the failure of the fast-projectile model leading to Eq. (4) is evident when $\Delta E\rightarrow\infty$ as $R\cos\theta\rightarrow 1$. The Barker-Berry model also fails as the projectile velocity increases, but does not have such a clear mathematical marker.

Devdariani *et al.*[7] calculated the amplitude for a discrete, autoionizing state interacting with the long-range field of an ion moving more slowly than the emitted electron. They applied the same method as Fano[20] for the interaction of a discrete state with a single continuum channel, but with a time-varying potential. In their case, this time-varying potential was the same as in the Barker-Berry model, and was $\Delta E=C[v(t'-t_0)]^{-1}$, where $C=-Q$, the charge of the ion times the charge of the electron. Their calculated amplitude is

$$f_r(\omega,\theta,E_p)=-i(\Gamma_r/2\pi)^{1/2}b_r(t_0,\theta,E_p)\times(\Delta\omega_r-\tfrac{1}{2}i\Gamma_r)^{-iC/v-1}\times\Gamma(1+iC/v)\exp(\pi C/2v+i\omega t_{0r})\,, \quad (5)$$

where $\Delta\omega_r=\omega-E_r$, $\Gamma(1+iC/v)$ is a complex gamma function, and $b_r(t_0,\theta,E_p)$ is the amplitude for excitation of the discrete state.

We have made a sign change so that Eq. (5) can reproduce Eq. (4.8) in the paper of Devdariani *et al.*[32] This equation, despite some confusion in their text, shows physically sensible behavior as a function of the parameters and is clearly correct. Some care must be taken, however, to properly define the quadrants of calculated inverse tangents.

It is important to understand, as has been discussed elsewhere,[17,7] that Eq. (5) is of more general applicability than many previous expressions for this amplitude,[1,4] in that it is valid both in the classically forbidden wing and in the limit when $C/v\rightarrow 0$.

Equation (5) may be used at higher projectile velocities with only two small modifications. First, the parameter C is made equal to $QR\cos\theta/(1-R\cos\theta)$ instead of $-Q$. Second, because there is always a large continuum that interferes quantum mechanically with the discrete peak, a coherent background amplitude a and an incoherent background intensity A are added. The spectrum, when summed over the relevant discrete states, is then

$$F(\omega,\theta,E_p)=A(\omega,\theta,E_p)+|\,a(\omega,\theta,E_p)+f(\omega,\theta,E_p)\,|^2 \quad (6)$$

$$=A+|\,a\,|^2+\sum_r\left\{\frac{\Gamma_r|\,b_r\,|^2}{(\Delta\omega_r)^2+\Gamma_r^2/4}\frac{C}{2v\sinh(\pi C/v)}\exp\left[\frac{\pi C}{v}-\frac{2C}{v}\tan^{-1}\left[\frac{\Gamma_r}{2\Delta\omega_r}\right]\right]\right.$$
$$+\left[\frac{\Gamma_r}{2\pi}\right]^{1/2}\frac{2|\,a\,|\,|\,b_r\,|}{(\Delta\omega_r)^2+\Gamma_r^2/4}|\,\Gamma(1+iC/v)\,|\exp\left[\frac{\pi C}{2v}-\frac{C}{v}\tan^{-1}\left[\frac{\Gamma_r}{2\Delta\omega_r}\right]\right]$$
$$\left.\times[\sin(\alpha_r)\Delta\omega_r+\cos(\alpha_r)\Gamma_r/2]\right\}\,, \quad (7)$$

where

$$\alpha_r = \frac{-C}{2v}\ln[(\Delta\omega_r)^2+\Gamma_r^2/4] + \arg[\Gamma(1+iC/v)]+\omega t_{0r} . \quad (8)$$

The spectral profile predicted by Eq. (7) may be highly asymmetric. This is due, in part, to the exponential term in Eq. (7) that is physically due to the acceleration (or deceleration) of the electron. Another interesting feature of the profile is due to the logarithmic term in the effective phase, α_r. This term, if C/v is large enough, may pass through multiples of 2π several times. This will cause oscillations of the peak profile. Such oscillations are characteristic of several PCI theories[4,9,6] that include interference between an autoionizing state and a continuum.

The solid lines in Figs. 1–3 are the result of a least-squares fit of the spectra using Eq. (7). The unknown parameters in Eq. (7) are A, $|a(\omega,\theta,E_p)|$, $|b_r(t_0,\theta,E_p)|$, E_r, and the initial phase shift, ωt_{0r}. A linear equation, $A=A+B\omega$, seemed adequate to fit the background over the energy range studied (30–43 eV). When doing the fit, Eq. (7) was numerically folded with a triangular spectrometer function that had a FWHM of 0.1 eV. As a test of the validity of Eq. (7), the value of C/v was allowed to vary as an adjustable parameter. The results are shown in Table I, where they are compared to the calculated values.

Two approximations made in Eq. (7) deserve some explanation. First, it is assumed that the discrete states interfere with one partial wave, and thus one phase, of the continuum. This is not generally the case since the emission peak interferes with all even and all odd partial waves.[21] Since, at any observation angle, there is still what may be called an "effective" phase difference between the state amplitudes and the continuum amplitude, this should not affect the validity of Eq. (7) as a parametrization. The unambiguous treatment of the parameters as the real physical quantities introduced above, however, is not legitimate.

TABLE I. A comparison of the calculated values of C/v $[=(Q/v)R\cos\theta/(1-R\cos\theta)]$ [see Eqs. (4) and (7)] to the values of C/v that resulted from least-squares fits, using Eq. (7), for the data presented in Figs. 1–3. The errors are statistical standard errors calculated by the fitting program.

	Fitted C/v	Calculated C/v
1500-keV Li^{3+} 20°	1.09±0.04	1.09
1500-keV Li^{3+} 40°	0.706±0.08	0.743
2000-keV He^{+} 30°	0.066±0.05	0.11
2000-keV He^{2+} 30°	0.112±0.03	0.22
3500-keV Li^{3+} 30°	0.310±0.03	0.303

Second, Eq. (7) ignores any possible interference between two adjacent autoionizing states. The $(2p^2)^1D$ and $(2s2p)^1P$ states are separated by 0.24 eV and have natural linewidths (FWHM) of about 0.073 and 0.039 eV, respectively. It is thus possible that they may interfere, especially when the natural linewidths are significantly broadened by PCI. The interference of adjacent autoionizing states has been problematic,[4,6] and perhaps a short aside on the proper representation of state-state interference is appropriate here.

The necessary and sufficient condition for interference is straightforward: two different processes begin from the same initial state and end up with indistinguishable final states. For the two autoionizing levels in question, it is possible that their excitation mechanisms are so different from each other that correlations may indeed be lost. Two obvious examples of this would be if excitation requires significantly different impact parameters or if one state requires electronic excitation of the projectile while the other state does not. The two states could then be distinguished by examination of the projectile, and when the projectile is not observed there would be no interference between the two states. If the excitation mechanisms are not that different, then the states will be partially correlated, and a fully general parametrization should take that into account.

An additional difficulty is due to the complicated nature of the interferences between the partial waves of the continuum and the discrete states.[21] This has the result that the single coherent continuum may have a different effective phase for autoionizing states of different angular momenta. Thus, while a best fit may uniquely determine the phase difference between the ^1P state and the continuum, and the phase difference between the ^1D state and the continuum, the phase difference between the ^1P state and the ^1D state will still not be known. This requires that an additional parameter, representing the state-state phase difference, be introduced into the parametric equation.

All of the above complications are eliminated if the state-state interference is relatively small. An estimate of the magnitude of this interference can indeed be calculated from Eq. (6) if two assumptions are made: (1) the two states (as is probably the case) are fully correlated, and (2) the state-state phase difference is determined by the state-continuum phase difference. Using these assumptions, the parameters resulting from the fit of the data in Fig. 1 were used to obtain an estimate of the interference effect. The results are shown in the inset of Fig. 1. The magnitude of the interference is very small, as shown here, and is typical of all spectra studied. It is clear that the quality of the data is not sufficient to distinguish between interference and no interference, and thus Eq. (7) is adequate to fit all our spectra.

It may be surprising that the magnitude of the state-state interference is so small when the state-continuum interference is so large. There is a simple mathematical reason for this. The size of an interference term is proportional to the product of the absolute magnitude of the two quantities in question. In the case of Fig. 1 the continuum amplitude is about 80 times larger than the ampli-

tude of the $(2s2p)^1P$ state. The state-state interference term is then about 80 times smaller than the $(2p^2)^1D$-to-continuum interference term. The continuum amplitude is, in addition, roughly constant over the relevant energy range, while the state amplitude, due to the $(\Delta\omega)^2+\Gamma^2/4$ term in the denominator, gets quite small away from the peak's resonance position. In slow-ion excitation of autoionizing states there is much less coherent background amplitude, and the peaks are often much distorted by PCI. For these reasons state-state interference may be considerably more significant.

In the limit when $C/v\rightarrow 0$, Eq. (7) reduces to

$$F(\omega,\theta,E_p)=A+|a|^2+\sum_r\left[\frac{(\Gamma_r/2\pi)|b_r|^2+(\Gamma_r/2\pi)^{1/2}|a|\,|b_r|\,\Gamma_r\cos(\omega t_{0r})}{(\Delta\omega_r)^2+\Gamma_r^2/4}+(\Gamma_r/2\pi)^{1/2}\frac{2|a|\,|b_r|\sin(\omega t_{0r})\Delta\omega}{(\Delta\omega_r)^2+\Gamma_r^2/4}\right], \tag{9}$$

which is clearly equivalent to the Shore parametrization [Eq. (1)]. In this case the asymmetric Shore parameter is

$$A_r=2(2/\Gamma_r\pi)^{1/2}|a|\,|b_r|\sin(\omega t_{0r}), \tag{10}$$

and the symmetric Shore parameter is

$$B_r=\frac{2|b_r|^2}{\Gamma_r\pi}+2(2/\Gamma_r\pi)^{1/2}|a|\,|b_r|\cos(\omega t_{0r}). \tag{11}$$

IV. CONCLUSION

A modification of a simple argument given previously[2] will serve to demonstrate the magnitude of the ion's field on the line profile. As we have seen, the energy shift at any time t, due to this "ionic dragging," is given in Eq. (2). The energy uncertainty at any time t, due to the uncertainty principle, is $\Delta E_u=1/(t-t_0)$. If, at any time t the magnitude of the dragging shift is the same as the magnitude of ΔE_u, the width of the peak will be dominated by the post-collision interaction, regardless of the lifetime of the state. This happens when the quantity

$$\frac{Q}{v}\frac{R\cos\theta}{1-R\cos\theta}\geq 1,$$

which, for $Q=1$ and $\theta=0$, happens at an atomic velocity of 2.3, or an energy of 132 keV/amu. Even when the condition in Eq. (12) fails, however, the post-collision dragging can be very significant. Note, for example, that in Fig. 2, where $C/v=0.81$, the oscillations in the spectral line shape can be explained by Eq. (7), but not by the Shore parametrization. In Fig. 3 the effect on the apparent width is easily visible to the eye as C/v varies from 0.11 to 0.34. Further evidence indicates[33] that quite small values of C/v, as small as 0.09, can change the direction of the profile asymmetry. In previous variants of the post-collision interaction theory, when the electron was considered much faster than the ion, a velocity of 1.0 a.u. was generally considered the upper velocity limit for significant post-collision effects.[2,17] It is apparent from the data and theory presented here that they must be included for velocities much faster than 1.0 a.u.

Previous observers[11–13,17] have commented on peculiar effects in this velocity regime when observing electrons emitted in the forward direction. No one, however, has commented on departures from a Beutler-Fano line profile, even though they may be observed in some of the measured spectral shapes.[12,16] Most attention has focused on the rapid variations of the profile parameters as functions of projectile energy and observation angle. The variations have been attributed to the effect of an ionic projectile on the formation of equal-velocity continuum states,[12,18,19] which is clearly separate and distinct. At forward angles the comparisons of theory[19] to various experiments[13,15,17] have been qualitative but not quantitative. We suggest that comparison will be more exact when the interaction of the ion with the emitted electron is included. A more complete experimental study in this kinematic regime, as well as comparison with theory, will be published shortly.[34]

It is interesting to speculate whether this type of post-collision interaction can be observed in other systems, in particular when atoms are excited by electrons that have after-collision velocities similar to the ion velocities studied in this paper. The theoretical treatment, however, would be more complicated. The kinematic situation is more difficult; the scattered electrons may have large scattering angles and their velocities will be significantly affected after autoionization of the helium atom by both the autoionized electron and the remnant ion. This effect has been assumed small in slow-electron PCI calculations,[4] where the position of the electron at the time of autoionization is the only significant factor. In this case, however, the relative velocity of the two electrons is also relevant, and a complete three-body calculation may be necessary. Interference between the scattered electrons and the autoionized electron must also be included. It should be straightforward to apply Eq. (7) to triply differential cross sections if the above effects are negligible: The angle θ becomes the angle between the two electrons, the sign of C is changed to account for the different projectile charge, and C should be divided by 2 to account for the equivalent masses of the two electrons. No such tests have been made on electron-scattering data.

ACKNOWLEDGMENTS

The author wishes to thank Hiroshi Kudo, Wolfram Stöffler, and Dino Zei for their experimental help, and Gordon Berry, Dieter Schneider, and Ugo Fano for their guidance. This research was performed at Argonne Na-

tional Laboratory under the auspices of the U.S. Department of Energy (Office of Basic Energy Sciences) under Contract No. W-31-109-Eng-38. The work was also performed while the author was supported by a program administered by the Argonne Division of Educational Programs with funding from the U.S. Department of Energy. This paper is submitted in partial fulfillment of the requirements for the Doctor of Philosophy degree, Department of Physics, Division of the Physical Sciences, University of Chicago.

---

*Present address: Joint Institute for Laboratory Astrophysics, University of Colorado, Boulder, CO 80302.

[1]R. B. Barker and H. W. Berry, Phys. Rev. **151**, 14 (1966).
[2]P. J. Hicks and J. Comer, J. Phys. B **8**, 1866 (1975).
[3]G. Gerber, R. Morgenstern, and A. Niehaus, J. Phys. B **6**, 493 (1973).
[4]R. Morgenstern, A. Niehaus, and U. Theilman, J. Phys. B **10**, 1039 (1977).
[5]C. G. King, F. H. Read, and R. C. Bradford, J. Phys. B **8**, 2210 (1975).
[6]F. H. Read, J. Phys. B **10**, L207 (1977).
[7]A. Z. Devdariani, V. W. Ostrovskii, and Yu. N. Sebyakin, Zh. Eksp. Teor. Fiz. **73**, 412 (1977) [Sov. Phys.—JETP **46**, 215 (1977)].
[8]G. N. Ogurtsov, Rev. Mod. Phys. **44**, 1 (1972).
[9]P. Dahl, M. Rødbro, B. Fastrup, and M. E. Rudd, J. Phys. B **9**, 1567 (1976).
[10]N. Stolterfoht, D. Schneider, D. Burch, B. Aagaard, E. Boving, and B. Fastrup, Phys. Rev. A **12**, 1313 (1975).
[11]A. Gleizes, P. Benoit-Cattin, A. Bordenave-Montesquieu, and H. Merchez, J. Phys. B **9**, 473 (1976).
[12]F. D. Schowengerdt and M. E. Rudd, Phys. Rev. Lett. **28**, 127 (1972).
[13]N. Stolterfoht, D. Ridder, and P. Ziem, Phys. Lett. **42A**, 240 (1972).
[14]D. Ridder, diplomarbeit, Freie Universität Berlin, 1973 (unpublished).
[15]A. Bordenave-Montesquieu, P. Benoit-Cattin, M. Rodiere, A. Gleizes, and H. Merchez, J. Phys. B **8**, 874 (1975).
[16]M. Prost, diplomarbeit, Freie Universität Berlin, 1978 (unpublished).
[17]A. Bordenave-Montesquieu, A. Gleizes, and P. Benoit-Cattin, Phys. Rev. A **25**, 245 (1982).
[18]S. S. Lipovetsky and V. S. Senashenko, J. Phys. B **7**, 693 (1974).
[19]V. N. Mileev, V. S. Senashenko, and E. Yu Tsymbal, J. Phys. B **14**, 2625 (1981).
[20]U. Fano, Phys. Rev. **124**, 1866 (1961).
[21]V. V. Balashov, S. S. Lipovetsky, and V. S. Senashenko, Zh. Eksp. Teor. Fiz. **63**, 1622 (1972) [Sov. Phys.—JETP **36**, 858 (1973)].
[22]V. V. Balashov, A. N. Grum-Grzhimailo, N. M. Kabachnik, A. I. Magunov, and S. I. Strakova, J. Phys. B **12**, (1979).
[23]J. Macek, Phys. Rev. A **1**, 235 (1970).
[24]M. E. Rudd, C. A. Sauter, and C. L. Baily, Phys. Rev. **151**, 20 (1966).
[25]K. D. Sevier, *Low Energy Electron Spectrometry* (Wiley-Interscience, New York, 1972).
[26]N. Stolterfoht, Hahn-Meitner-Insitut (Berlin) Bericht 104 (1971) (unpublished).
[27]B. W. Shore, J. Opt. Soc. Am. **57**, 881 (1967).
[28]R. J. Tweed, J. Phys. B **9**, 1725 (1976).
[29]W. Shearer-Izumi, At. Data Nucl. Data Tables **20**, 531 (1977).
[30]D. Bordenave-Montesquieu and R. Dagnac, J. Phys. B **12**, 1233 (1979).
[31]N. Stolterfoht, D. Brandt, and M. Prost, Phys. Rev. Lett. **43**, 1654 (1979).
[32]The version of Eq. (4.7) in the English translation of Ref. 7 is very different from the version in the Russian original.
[33]Distortion of He^{**} emission lines after fast-ion collisions, P. W. Arcuni, in Proceedings of the Workshop on Autoionization of Atoms and Small Molecules, Argonne, 1985 (unpublished).
[34]P. W. Arcuni (unpublished).